Archives of Gynecology and Obstetrics (2019) 299:1089–1098
https://doi.org/10.1007/s00404-018-5007-y

GYNECOLOGIC ONCOLOGY

E2F7, EREG, miR-451a and miR-106b-5p are associated with the cervical cancer development

Shan Zong[1] · **Xiaoxia Liu**[1] · **Na Zhou**[2] · **Ying Yue**[1]

Received: 14 June 2018 / Accepted: 7 December 2018 / Published online: 4 January 2019

Abstract

Purpose We aimed to seek the crucial genes or microRNAs (miRNA) correlated with the cervical cancer development.

Methods The miRNA profiling GSE30656 and gene expression profiling GSE63514 were obtained from Gene Expression Omnibus database. Differentially expressed microRNAs (DEMiRs) and differentially expressed genes (DEGs) were screened. Then target genes of DEMiRs were obtained and matched with DEGs to obtain interaction pairs between DEMiRs and DEGs. Gene Ontology-biological process and Kyoto Encyclopedia of Genes and Genomes (KEGG) pathway enrichment analyses were conducted for DEGs and DEMiRs in the DEMiRs–DEGs pairs. The DEMiRs–DEGs regulatory network, protein–protein interaction network and transcription factor (TF)–target regulatory network were constructed. Ultimately, long non-coding RNAs (lncRNAs) associated with DEMiRs were obtained, and then lncRNA–miRNA–target ceRNA network was established.

Results Total 18 DEMiRs and 620 DEGs were identified. DEMiRs were enriched in 35 KEGG pathways, such as PI3K–Akt signaling pathway (involving *miR-451a*). DEGs were enriched in various functions, such as DNA replication (involving *E2F7*) and angiogenesis (involving *EREG*). There were 120 nodes and 216 interaction pairs in the DEMIR–DEG regulatory network, and *miR-106b-5p* has the greatest degree. *EREG* and *E2F7* were regulated by *miR-451a* and *miR-148a-3p*, respectively. Besides, *E2F7* was identified in the TF–target regulatory network, regulating *CDC6*. There were 15 lncRNAs, 11 miRNAs and 90 DEGs in the ceRNA network. Specially, *miR-148a-3p* was interacted with lncRNA HOTAIR in the ceRNA network.

Conclusion *E2F7*, *EREG*, *miR-451a* and *miR-106b-5p* were likely to be related to the cervical cancer development.

Keywords Cervical cancer · Differentially expressed miRNAs · Differentially expressed genes · Regulatory network · Angiogenesis

Abbreviations

miRNA	MicroRNAs
DEGs	Differentially expressed genes
DEMiRs	Differentially expressed microRNAs
KEGG	Kyoto encyclopedia of genes and genomes
TFs	Transcription factors
lncRNAs	Long non-coding RNAs
GEO	Gene expression omnibus
BH	Benjamini and Hochberg
FC	Fold change
GO-BP	Gene ontology biological process
ORA	Enrichment analysis
NES	Normalized enrichment score
PCA	Principal component analysis
MAPK1	Mitogen-activated protein kinase 1

Introduction

Cervical cancer ranks second to breast cancer among women and endanger the health of women [1]. There are approximately 530,000 new cases of cervical cancer in 2008, and it is estimated to increase by 80% until 2020 without intensified prevention [2]. In particular, it shows that about 80% of cervical cancer occur in the developing countries because of the limited application of screening programs [3]. The life quality and health of women are severely affected by the cervical cancer.

✉ Ying Yue
fujiu15qiwen@163.com

[1] Department of Gynecology Oncology, The First Hospital of Jilin University, 71th Xinmin Road, Chang Chun 130021, Jilin, China

[2] Department of Gynecology and Obstetric, The First Hospital of Jilin University, Chang Chun 130021, Jilin, China

Several risk factors are associated with the occurrence of cervical cancer, such as human papillomavirus (HPV) infection [4] and smoking [5]. Of these factors, HPV infection is considered as the major risk factor for the occurrence of cervical cancer. It is reported that HPV types 16 and 18 accounts for 75% cervical cancer cases worldwide [1, 6]. Currently, microRNAs (miRNAs) have been proved to serve potential parts in the cervical cancer development. For example, previous study demonstrates that down-regulated *miR-214* has pivotal roles in facilitating cervical cancer pathogenesis [7]. The *miR-188* down-regulation and *miR-223* up-regulation are correlated with the short survival of cervical cancer patients [8]. *MiR-411* is down-regulated in cervical cancer samples and inhibits the development of cervical cancer through targeting signal transducer and activator of transcription 3 (*STAT3*) [9]. *MiR-146a* contributes to the cell viability of cervical cancer via targeting interleukin 1 receptor associated kinase 1 and TNF receptor associated factor 6 [10]. Additionally, several long non-coding RNAs (lncRNA) have also been identified to participate in the cervical cancer development. For example, lncRNA HOX transcript antisense RNA (*HOTAIR*) and *STAT3* synergistically regulate the migration and invasion of cervical cancer cells [11]. Despite of these findings, the detailed mechanism of cervical cancer remains unclear.

Wilting et al. integrated generated chromosomal profiles of the same samples and the genome-wide miRNA expression profiles of micro-dissected specimens of normal squamous epithelium, high-grade precancerous lesions, squamous cell carcinomas and adenocarcinomas in 2013 [12]. Den et al. analyzed the gene expressions of normal, precancerous, and cancerous cervical tissues, finding that the DNA replication/repair and cell proliferation genes are correlated with the cervical cancer development [13]. Nevertheless, they have not explored the detailed mechanisms of cervical cancer utilizing the comprehensive bioinformatics analyses. Here, the miRNA profiling GSE30656 [12] and gene expression profiling GSE63514 [13] were integrated to deeply seek the detailed mechanisms of cervical cancer. Differential expression analyses, enrichment analyses, protein–protein interaction (PPI) network analysis, and ceRNA network analysis were conducted. The study was expected to unravel the miRNAs, genes and pathways related to the cervical cancer development.

Materials and methods

Data source

The miRNA profiling GSE30656 was extracted from gene expression omnibus (GEO) database (http://www.ncbi.nlm.nih.gov/geo/), which was detected on the platform of Agilent-016436 Human miRNA Microarray 1.0. A total of ten squamous cell carcinomas of the cervix samples (including GSM760511, GSM760513, GSM760512, GSM760538, GSM760520, GSM760539, GSM760521, GSM760540, GSM760547, GSM760546) and ten cervical squamous epithelial samples (including GSM760508, GSM760510, GSM760507, GSM760542, GSM760509, GSM760541, GSM760548, GSM760550, GSM760543, GSM760549) with normal histology samples. The gene expression profiling GSE63514 was also obtained from GEO database, which contained 28 cervical squamous epithelial cancer samples and 24 normal cervical epithelium samples. All samples were detected through the (HG-U133_Plus_2) Affymetrix Human Genome U133 Plus 2.0 Array platform.

Data preprocessing, DEMiRs and DEGs identification

The obtained miRNA data were read and pre-processed utilizing the limma package (ver. 3.30.13, http://www.bioconductor.org/packages/release/bioc/html/limma.html) in R language (ver. 3.3.2) by conducting background correction, conversion of original data and expression levels calculation. Probes were annotated by the annotation file. If different probes were mapped to the same gene symbol, the average value of different probes would act as the final expression level of gene. We downloaded the raw CEL data and used the Oligo package (ver. 1.38.0, http://bioconductor.org/help/search/index.html?q=oligo/) [14] in R language to preprocess all the data by performing background correction, normalization, conversion of original data and quartile data normalization. The probes without matching gene symbols were filtered out, and the values of the probes corresponding to one gene were averaged to obtain the final gene expression value.

The non-paired *t* test method provided by limma package [15] was utilized for calculating the *p* values, and then the Benjamini and Hochberg (BH) method was applied to adjust the *p* values [16]. The adjusted *p* values < 0.05 and $|\log \text{fold change (FC)}| > 1$ were utilized as the threshold for screening differentially expressed miRNAs (DEMiRs). Meanwhile, the *p* values < 0.05 and $|\log \text{FC}| \geq 1$ were used as the threshold for identifying differentially expressed genes (DEGs).

Enrichment analyses

The target genes of miRNA were retrieved and predicted by the following 11 tools: miRWalk (http://zmf.umm.uni-heidelberg.de/apps/zmf/mirwalk2/) [17], Microt4, miRDB, miRanda, Pictar2, miRMap, PITA, miRNAMap, RNAhybrid, RNA22, and Targetscan. The target genes were selected if they can be predicted by more than eight retrieval tools among the above 11 tools. The

miRNA–target and DEGs were matched to obtain the interaction pairs between DEMiRs and DEGs.

The R package clusterProfiler (ver. 3.2.14, http://bioconductor.org/packages/release/bioc/html/clusterProfiler.html) [18] was utilized to perform the Kyoto encyclopedia of genes and genomes (KEGG) [19] pathway enrichment analysis for the miRNAs. The adjusted p values < 0.05 were the cut-off criteria for significant results. In addition, the gene ontology-biological process (GO-BP) [20] and KEGG pathway enrichment analyses for the DEGs in the DEMiR–DEG interaction pairs were implemented utilizing the overrepresentation enrichment analysis (ORA) method provided by the webgestal [21] (http://www.webgestalt.org/option.php) tool. Here, the p values < 0.05 were regarded as the threshold for significant results.

Regulatory network analyses

The Cytoscape software (ver. 3.6.0) [22] was used to establish the miRNA–gene regulatory network according to the interaction information of DEMiR–DEG. The Search Tool for the Retrieval of Interacting Genes (STRING) (ver. 10.0) database [23] was carried out to analyze the protein–protein interactions of DEGs in the DEMiR–DEG interaction pairs. The DEGs acted as the input gene set, while the Homo sapiens served as species. The PPI score was set as 0.4. Afterwards, the Cytoscape (ver. 3.6.0) software was applied to construct the PPI network.

The iRegulon (ver. 1.3, http://apps.cytoscape.org/apps/iRegulon) plugin [24] in Cytoscape was implemented to predict and analyze the interaction pairs of transcription factor (TF)–target gene in the PPI network. The parameters were set as follows: 0.001 act as the maximum false discovery rate on motif similarity, and 0.05 serve as the minimum identity among orthologous genes. The higher score of Normalized Enrichment Score (NES) in output results presented the more reliable results. The TF–target interaction pairs whose NES > 4 were selected for further study.

ceRNA network

The lncRNAs associated with miRNA were searched using the starBase tool (ver. 2.0, http://starbase.sysu.edu.cn/index.php) [25]. The searching parameters were set as follows: number of supporting experiments ≥ low stringency (≥ 1) and number of cancer types (Pan-Cancer) ≥ 1. Ultimately, the lncRNA–miRNA–target ceRNA network was established according to the interaction pairs among lncRAN–miRNA and miRNA–target.

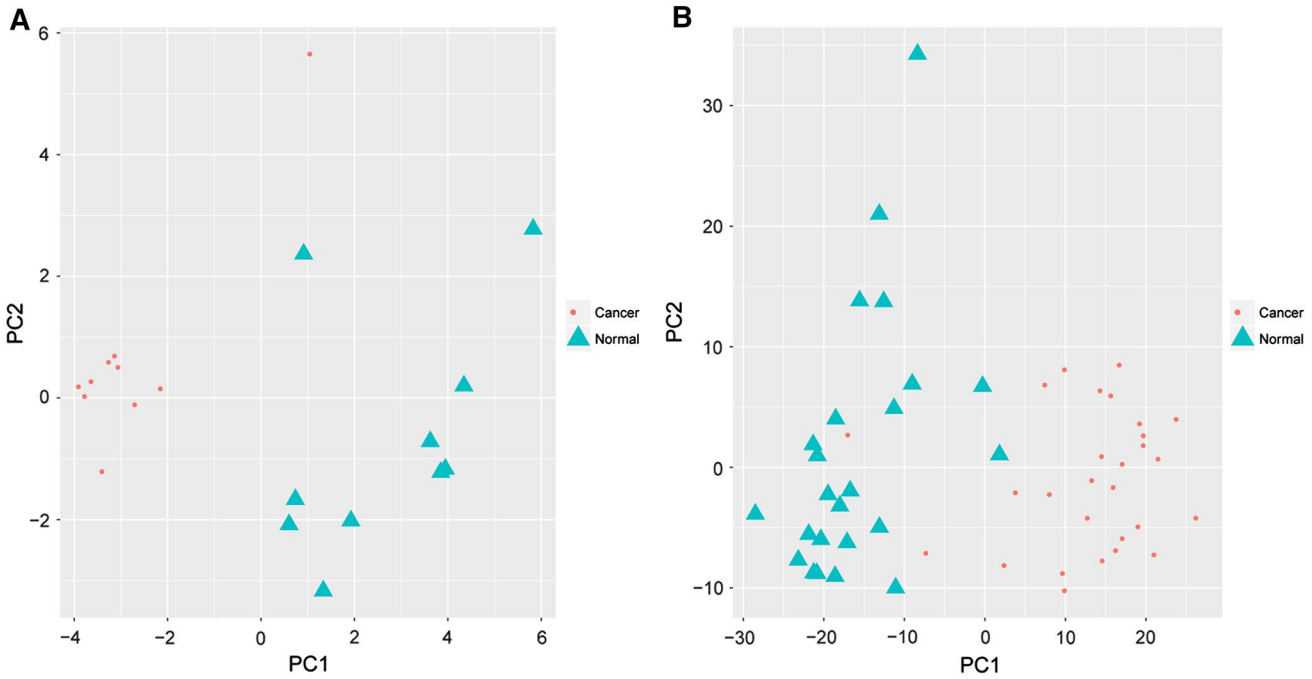

Fig. 1 PCA analysis for DEMiRs (**a**) and DEGs (**b**). Red color stands for the higher expression value, green color stands for the lower expression value. *DEGs* differentially expressed genes, *DEMiRs* differentially expressed microRNAs, *PCA* principal component analysis

Results

DEMiRs and DEGs identification

Total 18 DEMiRs were identified, including five up-regulated (e.g., *miR-106b-5p*) and 12 down-regulated DEMiRs (e.g., *miR-451a*, *miR-148a-3p*). Analogously, total 620 DEGs were obtained, including 286 up-regulated [e.g., E2F transcription factor 7 (*E2F7*)] and 334 down-regulated DEGs [e.g., epiregulin (*EREG*)]. The principal component analysis (PCA) results are presented in Fig. 1. Afterwards, 9200 target genes of the 18 miRNAs were obtained, and then 216 DEMiRs–DEGs interaction pairs were identified, including 5 up-regulated DEMiRs, 10 down-regulated DEMiRs, 57 up-regulated and 43 down-regulated DEGs.

Enrichment analysis

DEMiRs in the DEMiRs–DEGs pairs were enriched in 35 KEGG pathways (Fig. 2), such as beta-alanine metabolism, cysteine and methionine metabolism, and arginine and proline metabolism. Notably, *miR-451a* was enriched in the PI3K–Akt signaling pathway (Fig. 2). Up-regulated DEGs in the DEMiRs–DEGs pairs were enriched in five KEGG pathways, such as cell cycle, glutathione metabolism and leishmaniasis (Table 1). Down-regulated DEGs in the DEMiRs–DEGs pairs were enriched in seven KEGG pathways, such as prostate cancer, AGE–RAGE signaling pathway in diabetic complications, and ascorbate and aldarate metabolism (Table 1). Besides, the top ten enriched functions for up-regulated DEGs are listed in Table 2a, such as mitotic cell cycle process, mitotic nuclear division, and mitotic cell cycle. We found that *E2F7* was enriched in the function of DNA replication in this study. The top ten enriched functions for down-regulated DEGs are listed in

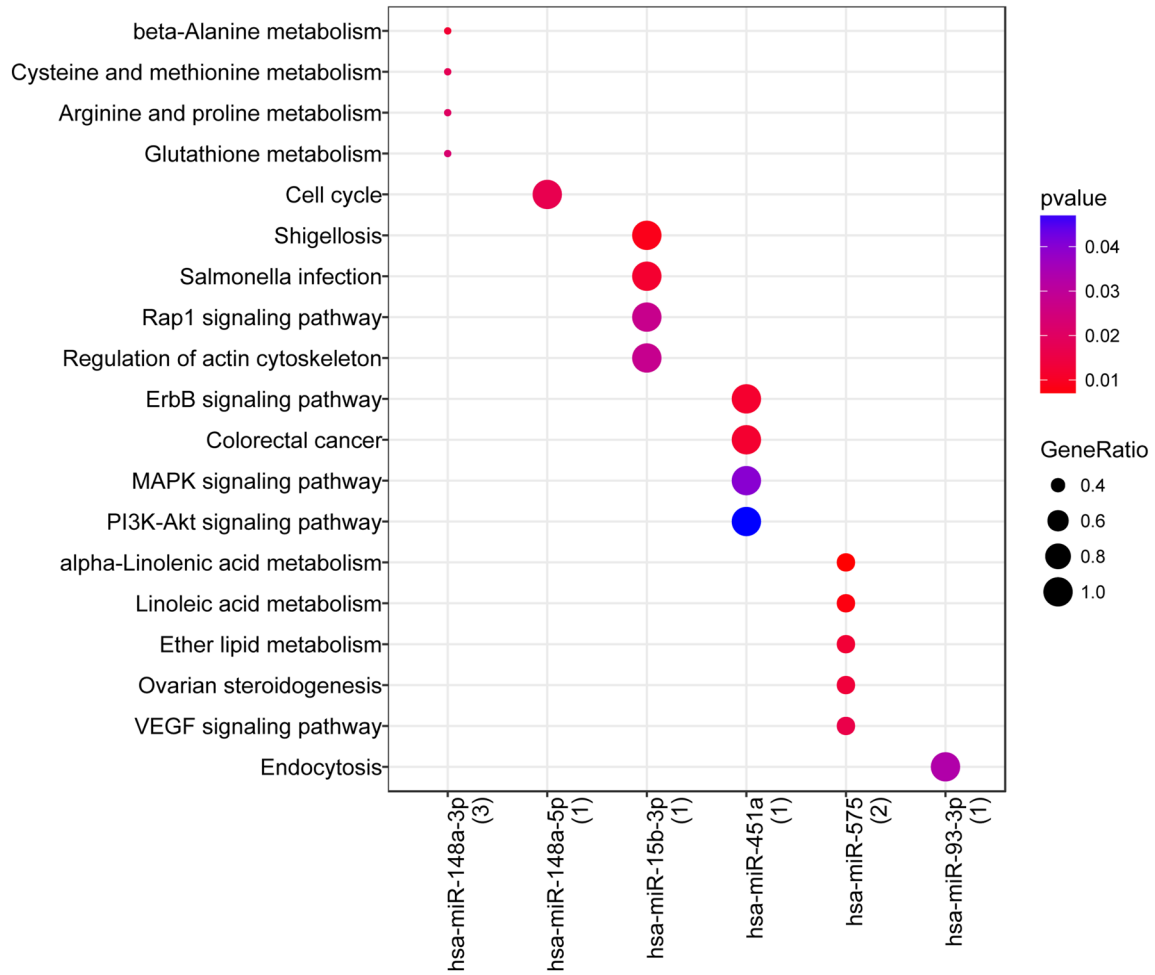

Fig. 2 KEGG pathway bubble diagram for DEMiRs. The darker color indicates the smaller *p* value. The bigger bubble indicates the significant pathway. *KEGG* Kyoto encyclopedia of genes and genomes, *DEMiRs* differentially expressed microRNAs

Table 1 KEGG pathway analysis for DEGs

Term	Description	Count	*p* value	Overlap gene
Up-regulated DEGs				
hsa04110	Cell cycle	119	8.79×10^{-4}	DBF4, CHEK1, CDC6, CDC25B
hsa00480	Glutathione metabolism	45	1.20×10^{-2}	RRM2, SMS
hsa05140	Leishmaniasis	60	2.07×10^{-2}	MARCKSL1, STAT1
hsa04115	P53 signaling pathway	67	2.54×10^{-2}	CHEK1, RRM2
hsa00982	Drug metabolism—cytochrome P450	46	4.68×10^{-3}	FMO2, UGT2B17
Down-regulated DEGs				
hsa05215	Prostate cancer	87	1.60×10^{-2}	AR, CCND1
hsa04933	AGE–RAGE signaling pathway in diabetic complications	99	2.05×10^{-2}	F3, CCND1
hsa00053	Ascorbate and aldarate metabolism	13	2.91×10^{-2}	UGT2B17
hsa04550	Signaling pathways regulating pluripotency of stem cells	135	3.64×10^{-2}	ISL1, KLF4
hsa00040	Pentose and glucuronate interconversions	18	4.01×10^{-2}	UGT2B17
hsa04921	Oxytocin signaling pathway	149	4.36×10^{-2}	PLA2G4A, CCND1
hsa00592	Alpha-linolenic acid metabolism	20	4.45×10^{-2}	PLA2G4A

KEGG Kyoto encyclopedia of genes and genomes, *DEGs* differentially expressed genes

Table 2b, such as epidermis development, skin development, and epidermal cell differentiation. In particular, we found that *EREG* was enriched in the function of angiogenesis.

DEMIR–DEG regulatory network

There were 120 nodes and 216 interaction pairs in the DEMiR–DEG regulatory network (Fig. 3a). The top ten DEMiRs and DEGs are presented in Table 3a, b. Here, *miR-106b-5p* has the greatest degree in the DEMiR–DEG regulatory network. *EREG* and *E2F7* were regulated by

Table 2 The top ten GO-BP function analyses for DEGs

Term	Description	Count	*p* value	Overlap gene
(a) Up-regulated DEGs				
GO:1903047	Mitotic cell cycle process	843	3.89×10^{-10}	DBF4, CHEK1, etc
GO:0007067	Mitotic nuclear division	409	1.60×10^{-9}	CHEK1, CDC6, etc
GO:0000278	Mitotic cell cycle	924	1.70×10^{-9}	DBF4, CHEK1, etc
GO:0000280	Nuclear division	539	4.57×10^{-9}	CHEK1, CDC6, etc
GO:0000910	Cytokinesis	117	8.60×10^{-9}	E2F7, CDC6, etc
GO:0048285	Organelle fission	579	1.14×10^{-8}	CHEK1, CDC6, etc
GO:0000281	Mitotic cytokinesis	30	6.83×10^{-8}	KIF4A, ANLN, etc
GO:0022402	Cell cycle process	1225	1.37×10^{-7}	DBF4, CHEK1, etc
GO:0061640	Cytoskeleton-dependent cytokinesis	38	2.35×10^{-7}	KIF23, CDC6, etc
GO:0051301	Cell division	518	2.42×10^{-7}	E2F7, CDC6, etc
(b) Down-regulated DEGs				
GO:0008544	Epidermis development	263	4.38×10^{-6}	EMP1, EREG, etc
GO:0043588	Skin development	210	1.53×10^{-5}	EREG, PPL, etc
GO:0009913	Epidermal cell differentiation	151	4.17×10^{-5}	EREG, PPL, etc
GO:0048730	Epidermis morphogenesis	30	6.25×10^{-5}	TMEM79, KLF4, etc
GO:0030216	Keratinocyte differentiation	105	1.53×10^{-4}	EREG, PPL, etc
GO:0030855	Epithelial cell differentiation	520	3.32×10^{-4}	EREG, AR, etc
GO:0033327	Leydig cell differentiation	11	3.56×10^{-4}	AR, CCND1, etc
GO:0061180	Mammary gland epithelium development	60	4.99×10^{-4}	AR, CCND1, etc
GO:0060749	Mammary gland alveolus development	16	7.70×10^{-4}	AR, CCND1, etc
GO:0061377	Mammary gland lobule development	16	7.70×10^{-4}	AR, CCND1

DEGs differentially expressed genes, *GO-BP* gene ontology biological process

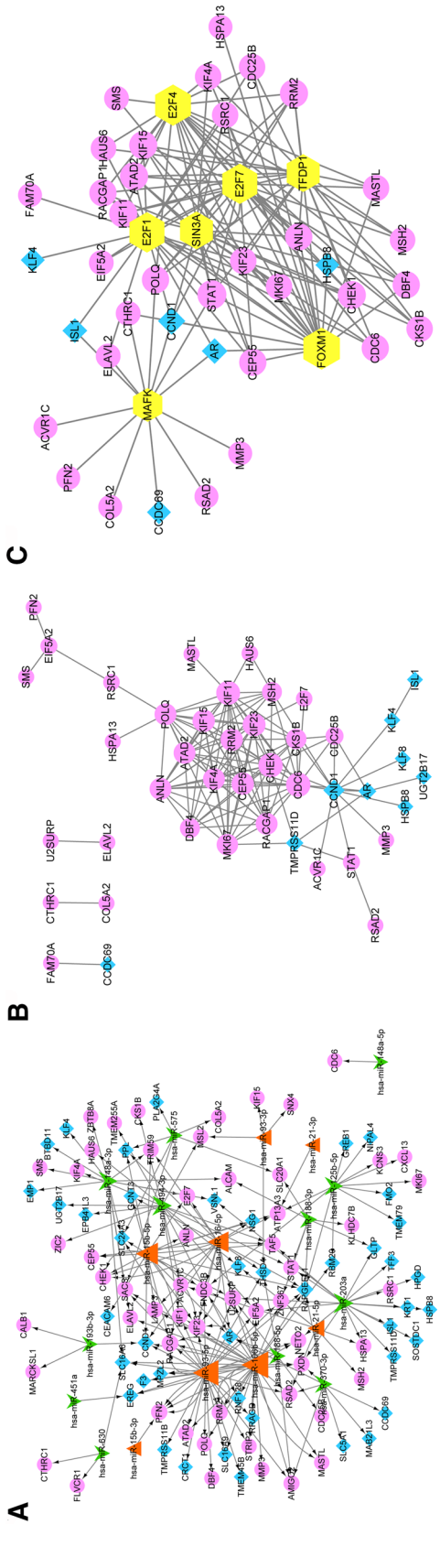

Fig. 3 DEMiRs–DEGs regulatory network (**a**), PPI network (**b**) and TF–target regulatory network (**c**). **a** DEMiRs–DEGs regulatory network for DEMiRs and DEGs. Orange triangles and green arrows represent the up-regulated DEMiRs and down-regulated DEMiRs, respectively. Pink rounds and light blue rhombus represent up-regulated and down-regulated DEGs, respectively. The arrows present the regulatory direction. **b** PPI network for DEMiRs and DEGs. Pink rounds and light blue rhombus represent up-regulated and down-regulated DEGs, respectively. The size of nodes presents the value of degree. The larger nodes indicate a larger degree value. **c** TF–target regulatory network. Pink rounds and light blue rhombus represent up-regulated and down-regulated DEGs, respectively. Yellow hexagons stand for the TFs. The size of nodes presents the value of degree. The larger nodes indicate a larger degree value. *DEMiRs* differentially expressed microRNAs, *DEGs* differentially expressed genes, *PPI* protein–protein interaction, *TFs* transcription factors

Table 3 The top ten DEMiRs/DEGs in the regulatory network

Nodes	Degree	Description
(a) DEMiRs in the DEMiR–DEG regulatory network		
hsa-miR-106b-5p	38	Up
hsa-miR-93-5p	34	Up
hsa-miR-15b-5p	23	Up
hsa-miR-16-5p	19	Up
hsa-miR-203a	17	Down
hsa-miR-494-3p	15	Down
hsa-miR-148a-3p	13	Down
hsa-miR-125b-5p	11	Down
hsa-miR-370-3p	8	Down
hsa-miR-188-3p	7	Down
(b) DEGs in the DEMiR–DEG regulatory network		
RAPGEFL1	7	Down
KIF23	7	Up
FNDC3B	6	Up
U2SURP	6	Up
RACGAP1	6	Up
CCND1	5	Down
AR	5	Down
PFN2	5	Up
SLC16A6	4	Down
SLC24A3	4	Down

DEGs differentially expressed genes, *DEMiRs* differentially expressed microRNAs

miR-451a and *miR-148a-3p*, respectively (Fig. 3a). The PPI network was constructed and is showed in Fig. 3b. A total of 43 nodes and 136 interaction pairs were contained in the PPI network. The top ten DEGs are presented in Table 3b. In addition, seven TFs were predicted in the PPI network by the iRegulon software. Then 133 regulatory interaction pairs of TFs–target were obtained, including 32 up-regulated and six down-regulated targets. The TF–target regulator network is shown in Fig. 3c. Here, *E2F7* was identified in the TF–target regulatory network, regulating cell division cycle protein 6 (*CDC6*).

ceRNA network

A total of 45 lncRNA–miRNA interaction pairs were obtained through the starBase tool. *MiR-148a-3p* was interacted with lncRNA *HOTAIR* in our study. Furthermore, 11 DEMiRs simultaneously associated with lncRNAs and target genes were screened, of these, five were up-regulated (e.g., *E2F7*) and six were down-regulated. Moreover, 15 lncRNAs and 90 DEGs (including 48 up-regulated and 42 down-regulated DEGs) were also obtained. The ceRNA network is shown in Fig. 4.

Discussion

Totally, 18 DEMiRs and 620 DEGs were identified in this study. DEMiRs were enriched in 35 KEGG pathways, such as PI3K–Akt signaling pathway (involving *miR-451a*). DEGs were enriched in various functions, such as DNA replication (involving *E2F7*) and angiogenesis (involving *EREG*). There were 120 nodes and 216 interaction pairs in the DEMiR–DEG regulatory network, and *miR-106b-5p* has the greatest degree. *EREG* and *E2F7* were regulated by *miR-451a* and *miR-148a-3p*, respectively. Besides, *E2F7* was identified in the TF–target regulatory network, regulating *CDC6*. There were 15 lncRNAs, 11 DEMiRs and 90 DEGs in the ceRNA network. Specially, *miR-148a-3p* was interacted with lncRNA *HOTAIR* in the ceRNA network.

To the best of our knowledge, angiogenesis promotes the metastasis, growth and development of cancers [26]. It has been demonstrated that enhanced angiogenesis is closely related to the metastasis and development of cervical cancer [27, 28]. Recently, A-kinase interacting protein 1 has been found to play crucial parts in cervical cancer angiogenesis via increasing the expressions of C–X–C motif chemokine ligand 1 (*CXCL1*), *CXCL2*, and *CXCL8* [29]. These results suggested that genes associated with the cervical cancer angiogenesis might be related to the cervical cancer development. *EREG* was down-regulated in cervical cancer samples and enriched in the angiogenesis function in this study. Therefore, we speculated that *EREG* was likely to be related to the cervical cancer progression via regulating the angiogenesis process.

It has been uncovered that *miR-451* plays a vital role in a variety of human cancers, such as bladder cancer and osteosarcoma [30–32]. Nevertheless, the role of *miR-451* in cervical cancer has not been explored. *MiR-451a* was down-regulated in cervical cancer samples and enriched in the PI3K–Akt signaling pathways in this study. PI3K–Akt signaling pathway has pivotal roles in the proliferation, apoptosis and autophagy of cervical cancer cells [33, 34]. Recently, Li et al. indicate that S100 calcium binding protein A6 facilitates the migration and proliferation of cervical cancer cells by the activation of PI3K–Akt signaling pathway [35]. Nuclear factor 90 facilitates the angiogenesis of cervical cancer by regulating hypoxia inducible factor 1 alpha subunit/vascular endothelial growth factor A expression through participating in the PI3K–Akt signaling pathway [36]. These findings suggested that PI3K–Akt signaling pathway may participate in the cervical cancer progression. In addition, we found that EREG was regulated by *miR-451a*, which might participate in the cervical cancer progression. Thus, *miR-451a* was likely to be related to the cervical

cancer progression by regulating the PI3K–Akt signaling pathway and *EREG*.

Here, *E2F7* was up-regulated in cervical cancer samples and enriched in the function of DNA replication. It has been showed that DNA replication affects cell proliferation, tumorigenesis and progression [37, 38]. Liu et al. reveal that the up-regulation of sine oculis homeobox homolog 1 contributes to the invasive growth, tumorigenesis, and progression of cervical cancer via facilitating DNA replication [39]. In this case, the up-regulation of *E2F7* might participate in the cervical cancer development via modulating DNA replication function. Intriguingly, *E2F7* was identified in the TF–target regulatory network, regulating *CDC6* gene. *CDC6* expression is significantly related to the metastasis and invasion of cervical cancer [40]. Therefore, *E2F7* was likely to be associated with the cervical cancer development through regulating the expression of *CDC6*.

Numerous studies have revealed that *miR-106b* participates in the regulation of migration and invasion in a variety of human cancers, such as melanoma [41–43]. *MiR-106b* overexpression regulated by transforming growth factor beta 1 dramatically contributes to the cell migration in cervical cancer by targeting *DAB2* [44]. *MiR-106b* is involved in the regulation of EMT processes of cervical cancer cell lines HeLa and SiHa [45]. Gao and his colleagues demonstrate that *miR-106b-5p* expression is higher in cervical cancer samples compared with normal samples [46]. Here, the *miR-106b-5p* was up-regulated in cervical cancer samples and has the greatest degree in the DEMiR–DEG regulatory network. These results revealed that *miR-106b-5p* might be related to the cervical cancer development.

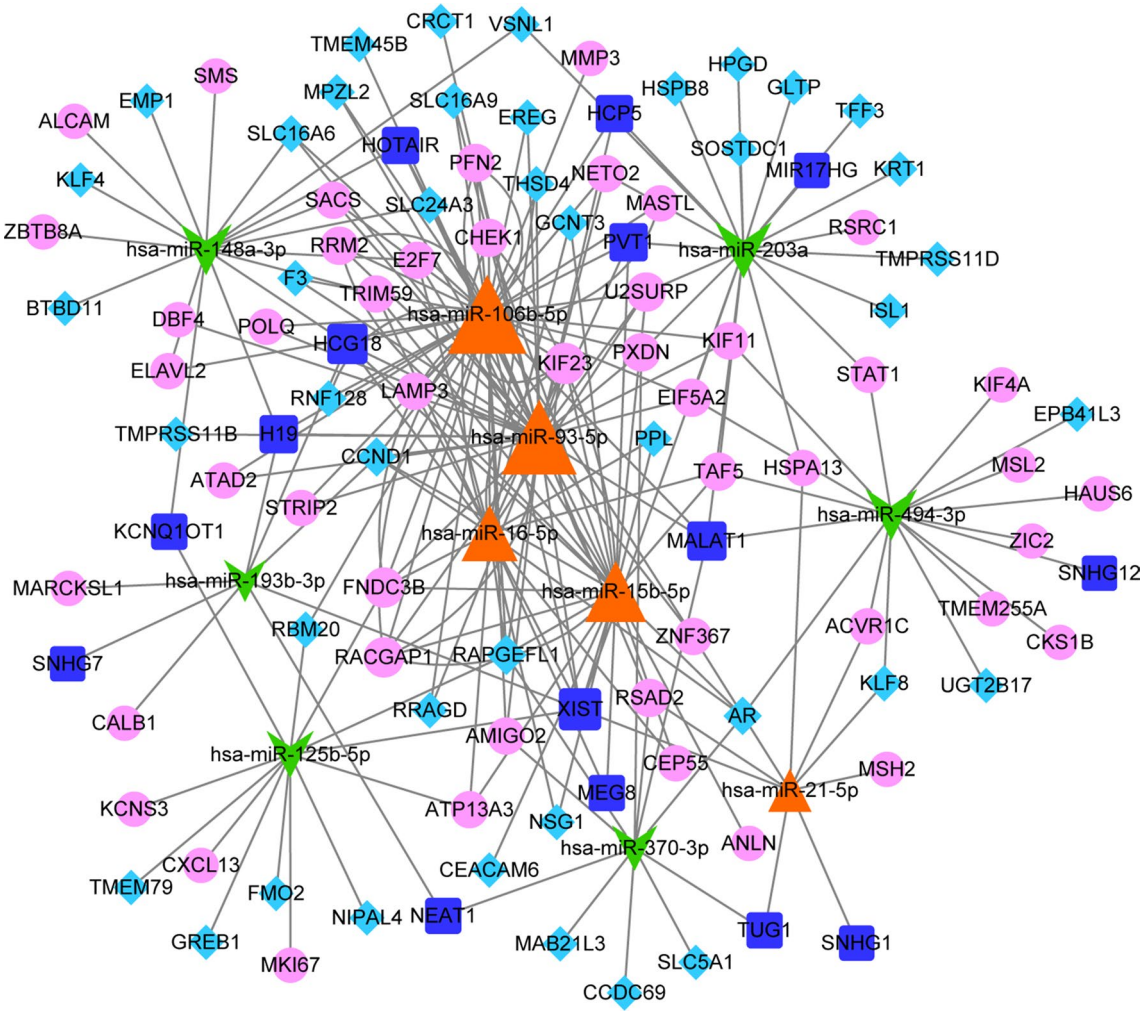

Fig. 4 The ceRNA regulatory network for DEMiRs, DEGs and lncRNAs. Orange triangles and green arrows represent the up-regulated DEMiRs and down-regulated DEMiRs, respectively. Pink rounds and light blue quadrangles represent up-regulated and down-regulated DEGs, respectively. Mazarine squares represent lncRNAs. The size of nodes stands for the nodes degree, and the large nodes have higher degrees. *DEMiRs* differentially expressed microRNAs, *DEGs* differentially expressed genes, *lncRNAs* long non-coding RNAs

LncRNA *HOTAIR* up-regulation is found in cervical cancer cells [11]. The elevated expression of lncRNA *HOTAIR* facilitates the growth of cervical cancer cell through promoting the *BCL2* expression regulated by *miR-143-3p* [47]. The up-regulation of lncRNA *HOTAIR* contributes to the metastasis and proliferation of cervical cancer by competitively binding *miR-23b* and regulating mitogen-activated protein kinase 1 (*MAPK1*) [48]. Here, *miR-148a-3p* was down-regulated in cervical cancer samples and interacted with lncRNA *HOTAIR* in our study. *E2F7* was up-regulated in cervical cancer samples and regulated by *miR-148a-3p*. Hence, LncRNA *HOTAIR* might function as a ceRNA via sponging with *miR-148a-3p* to up-regulate *E2F7* expression.

Conclusion

In summary, *E2F7*, *EREG*, *miR-451a* and *miR-106b-5p* were likely to be related to the cervical cancer development. These molecular markers might be useful for an early diagnosis and prognosis of cervical cancer. However, the predicted results cannot be verified by laboratory data, and further detailed investigation should be required.

Author contributions SZ and YY contributed to the conceptualization. XL and NZ acquired and interpreted the data. SZ explained some important intellectual content and drafted the manuscript. YY revised the manuscript and is responsible for the further intellectual explanation and correspondence.

Compliance with ethical standards

Ethical statement Not applicable.

Conflict of interest The authors report no conflict of interest.

References

1. Petry K (2014) HPV and cervical cancer. Scand J Clin Lab Invest Suppl 244:59–62 **(discussion 62)**
2. Arbyn M, Castellsagué X, de Sanjosé S, Bruni L, Saraiya M, Bray F, Ferlay J (2011) Worldwide burden of cervical cancer in 2008. Ann Oncol 22(12):2675–2686
3. Kent A (2010) HPV vaccination and testing. Rev Obstet Gynecol 3(1):33–34
4. Bosch FX, Lorincz A, Muñoz N, Meijer CJLM, Shah KV (2002) The causal relation between human papillomavirus and cervical cancer. J Clin Pathol 55(4):244–265
5. Gadducci A, Barsotti C, Cosio S, Domenici L, Riccardo Genazzani A (2011) Smoking habit, immune suppression, oral contraceptive use, and hormone replacement therapy use and cervical carcinogenesis: a review of the literature. Gynecol Endocrinol 27(8):597–604
6. Zur-Hausen H (2009) Papillomaviruses in the causation of human cancers—a brief historical account. Virology 384(2):260–265
7. Wang F, Tan W, Liu W, Jin Y, Dong D, Zhao X, Liu Q (2018) Effects of miR-214 on cervical cancer cell proliferation, apoptosis and invasion via modulating PI3K/AKT/mTOR signal pathway. Eur Rev Med Pharmacol Sci 22(7):1891–1898
8. Gao C, Zhou C, Zhuang J, Liu L, Liu C, Li H, Liu G, Wei J, Sun C (2018) MicroRNA expression in cervical cancer: novel diagnostic and prognostic biomarkers. J Cell Biochem 119(8):7080–7090
9. Shan D, Shang Y, Hu T (2018) MicroRNA-411 inhibits cervical cancer progression by directly targeting STAT3. Oncol Res. https://doi.org/10.3727/096504018X15247361080118
10. Hu Q, Song J, Ding B, Cui Y, Liang J, Han S (2018) miR-146a promotes cervical cancer cell viability via targeting IRAK1 and TRAF6. Oncol Rep 39(6):3015–3024
11. Zhang Y, Cheng X, Liang H, Jin Z (2018) Long non-coding RNA HOTAIR and STAT3 synergistically regulate the cervical cancer cell migration and invasion. Chem Biol Interact 286:106–110
12. Wilting S, Snijders P, Verlaat W, Jaspers A, van de Wiel M, van Wieringen W, Meijer G, Kenter G, Yi Y, le Sage C, Agami R, Meijer C, Steenbergen R (2013) Altered microRNA expression associated with chromosomal changes contributes to cervical carcinogenesis. Oncogene 32(1):106–116
13. den Boon J, Pyeon D, Wang S, Horswill M, Schiffman M, Sherman M, Zuna R, Wang Z, Hewitt S, Pearson R, Schott M, Chung L, He Q, Lambert P, Walker J, Newton M, Wentzensen N, Ahlquist P (2015) Molecular transitions from papillomavirus infection to cervical precancer and cancer: role of stromal estrogen receptor signaling. Proc Natl Acad Sci USA 112(25):E3255–E3264
14. Carvalho BS, Irizarry RA (2010) A framework for oligonucleotide microarray preprocessing. Bioinformatics 26(19):2363–2367. https://doi.org/10.1093/bioinformatics/btq431
15. Smyth GK (2005) limma: Linear models for microarray data. In: Gentleman R, Carey VJ, Huber W, Irizarry RA, Dudoit S (eds) Bioinformatics and computational biology solutions using R and bioconductor. Statistics for biology and health. Springer, New York, NY. https://doi.org/10.1007/0-387-29362-0_23
16. Benjamini Y, Hochberg Y (1995) Controlling the false discovery rate—a practical and powerful approach to multiple testing. J R Stat Soc 57(1):289–300
17. Dweep H, Gretz N (2015) miRWalk2.0: a comprehensive atlas of microRNA–target interactions. Nat Methods 12(8):697. https://doi.org/10.1038/nmeth.3485. http://www.nature.com/nmeth/journal/v12/n8/abs/nmeth.3485.html#supplementary-information
18. Yu G, Wang LG, Han Y, He QY (2012) clusterProfiler: an R package for comparing biological themes among gene clusters. Omics J Integr Biol 16(5):284–287
19. Kanehisa M, Goto S (2000) KEGG: Kyoto encyclopedia of genes and genomes. Nucleic Acids Res 27(1):29–34
20. Sherlock G (2009) Gene Ontology: tool for the unification of biology. Can Inst Food Sci Technol J 22(4):415
21. Zhang B, Kirov S, Snoddy J (2005) WebGestalt: an integrated system for exploring gene sets in various biological contexts. Nucleic Acids Res 33(web server issue):741–748
22. Shannon P, Markiel A, Ozier O, Baliga NS, Wang JT, Ramage D, Amin N, Schwikowski B, Ideker T (2003) Cytoscape: a software environment for integrated models of biomolecular interaction networks. Genome Res 13(11):2498–2504. https://doi.org/10.1101/gr.1239303
23. Szklarczyk D, Franceschini A, Kuhn M, Simonovic M, Roth A, Minguez P, Doerks T, Stark M, Muller J, Bork P (2011) The STRING database in 2011: functional interaction networks of proteins, globally integrated and scored. Nucleic Acids Res 39(database issue):561–568
24. Janky RS, Verfaillie A, Imrichová H, Sande BVD, Standaert L, Christiaens V, Hulselmans G, Herten K, Sanchez MN, Potier

D (2014) iRegulon: from a gene list to a gene regulatory network using large motif and track collections. PLoS Comput Biol 10(7):e1003731
25. Li JH, Liu S, Zhou H, Qu LH, Yang JH (2014) starBase v2.0: decoding miRNA–ceRNA, miRNA–ncRNA and protein–RNA interaction networks from large-scale CLIP-Seq data. Nucleic Acids Res 42(database issue):92
26. Folkman J (1992) Angiogenesis. J Biol Chem 267(16):1–18
27. Landt S, Mordelt K, Schwidde I, Barinoff J, Korlach S, Stãblen F, Lichtenegger W, Sehouli J, Kãmmel S (2011) Prognostic significance of the angiogenic factors angiogenin, endoglin and endostatin in cervical cancer. Anticancer Res 31(8):2651–2655
28. Liu H, Xiao J, Yang Y, Liu Y, Ma R, Li Y, Deng F, Zhang Y (2011) COX-2 expression is correlated with VEGF-C, lymphangiogenesis and lymph node metastasis in human cervical cancer. Microvasc Res 82(2):131–140
29. Zhang W, Wu Q, Wang C, Yang L, Liu P, Ma C (2018) AKIP1 promotes angiogenesis and tumor growth by upregulating CXC-chemokines in cervical cancer cells. Mol Cell Biochem 1:1–10
30. Zeng T, Peng L, Chao C, Fu B, Wang G, Wang Y, Zhu X (2014) miR-451 inhibits invasion and proliferation of bladder cancer by regulating EMT. Int J Clin Exp Pathol 7(11):7653–7662
31. Liu X, Zhang A, Xiang J, Lv Y, Zhang X (2016) miR-451 acts as a suppressor of angiogenesis in hepatocellular carcinoma by targeting the IL-6R-STAT3 pathway. Oncol Rep 36(3):1385–1392
32. Xu H, Mei Q, Shi L, Lu J, Zhao J, Fu Q (2014) Tumor-suppressing effects of miR451 in human osteosarcoma. Cell Biochem Biophys 69(1):163–168
33. Qian S, Li M (2017) Chamaejasmine induces apoptosis in HeLa cells through the PI3K/Akt signaling pathway. Anticancer Drugs 28(1):40
34. Jeyamohan S, Moorthy RK, Kannan MK, Arockiam AJV (2016) Parthenolide induces apoptosis and autophagy through the suppression of PI3K/Akt signaling pathway in cervical cancer. Biotech Lett 38(8):1251–1260
35. Li A, Gu Y, Li X, Sun H, Zha H, Xie J, Zhao J, Huang M, Chen L, Peng Q (2018) S100A6 promotes the proliferation and migration of cervical cancer cells via the PI3K/Akt signaling pathway. Oncol Lett 15(4):5685–5693
36. Zhang W, Xiong Z, Wei T, Li Q, Tan Y, Ling L, Feng X (2018) Nuclear factor 90 promotes angiogenesis by regulating HIF-1α/VEGF-A expression through the PI3K/Akt signaling pathway in human cervical cancer. Cell Death Dis 9(3):276
37. Mazurek A, Luo W, Krasnitz A, Hicks J, Powers RS, Stillman B (2012) DDX5 regulates DNA replication and is required for cell proliferation in a subset of breast cancer cells. Cancer Discov 2(9):812
38. Costa A, Hood IV, Berger JM (2013) Mechanisms for initiating cellular DNA replication. Annu Rev Biochem 82(82):25
39. Liu D, Zhang XX, Xi BX, Wan DY, Li L, Zhou J, Wang W, Ma D, Wang H, Gao QL (2014) Sine oculis homeobox homolog 1 promotes DNA replication and cell proliferation in cervical cancer. Int J Oncol 45(3):1232
40. Wang WX, Zhang WJ, Peng ZL, Yang KX (2009) Expression and clinical significance of CDC6 and hMSH2 in cervical carcinoma. J Sichuan Univ 40(5):857–860
41. Yang TS, Yang XH, Chen X, Wang XD, Hua J, Zhou DL, Zhou B, Song ZS (2014) MicroRNA-106b in cancer-associated fibroblasts from gastric cancer promotes cell migration and invasion by targeting PTEN. FEBS Lett 588(13):2162–2169
42. Song E (2013) MiR-106b expression determines the proliferation paradox of TGF-|[beta]| in breast cancer cells. Oncogene 34(1):84–93
43. Prasad R, Katiyar SK (2014) Down-regulation of miRNA-106b inhibits growth of melanoma cells by promoting G1-phase cell cycle arrest and reactivation of p21/WAF1/Cip1 protein. Oncotarget 5(21):10636–10649
44. Cheng Y, Guo Y, Zhang Y, You K, Li Z, Geng L (2016) MicroRNA-106b is involved in transforming growth factor β1-induced cell migration by targeting disabled homolog 2 in cervical carcinoma. J Exp Clin Cancer Res 35(1):1–11
45. Piao J, You K, Guo Y, Zhang Y, Li Z, Geng L (2017) Substrate stiffness affects epithelial–mesenchymal transition of cervical cancer cells through miR-106b and its target protein DAB2. Int J Oncol 50(6):2033–2042
46. Gao D, Zhang Y, Zhu M, Liu S, Wang X (2016) miRNA expression profiles of HPV-infected patients with cervical cancer in the Uyghur population in China. PLoS ONE 11(10):e0164701
47. Liu M, Jia J, Wang X, Liu Y, Wang C (2018) Long non-coding RNA HOTAIR promotes cervical cancer progression through regulating BCL2 via targeting miR-143-3p. Cancer Biol Ther 19:1–9
48. Li Q, Feng Y, Chao X, Shi S, Liang M, Qiao Y, Wang B, Wang P, Zhu Z (2018) HOTAIR contributes to cell proliferation and metastasis of cervical cancer via targeting miR-23b/MAPK1 axis. Biosci Rep 38(1):BSR20171563